

## Time correlated single photon Mie scattering from a sonoluminescing bubble

K. R. Weninger,<sup>1</sup> P. G. Evans,<sup>2</sup> and S. J. Putterman<sup>1</sup>

<sup>1</sup>Department of Physics, University of California, Los Angeles, California 90095

<sup>2</sup>Division of Engineering and Applied Sciences, Harvard University, Cambridge, Massachusetts 02138

(Received 7 October 1999)

Application of time correlated single photon counting to pulsed Mie scattering enables one to resolve changes in light scattering to better than 50 ps. This technique is applied to the highly nonlinear motion of a sonoluminescing bubble. Physical processes, such as outgoing shock wave emission, that limit the interpretation of the data are measured with a streak camera and microscopy. Shock speeds about 6 km/s have been observed.

PACS number(s): 78.60.Mq, 42.68.Mj, 43.25.+y

The acoustically driven pulsations of a gas bubble in water can be so nonlinear as to generate broad band ultraviolet flashes of light, which, depending on the system, last from 35 to 350 ps [1,2]. This energy focusing phenomenon known as sonoluminescence (SL) results from the runaway collapse of a bubble which was first studied theoretically in connection with cavitation damage by Rayleigh [3]. The singularity which develops as a result of the bubble collapse presents not only a difficult modeling problem [4] but has also proved challenging to measure experimentally [5–8]. CW light scattering methods have been effective in measuring the dynamical response of the bubble to the driving sound for all phases of the motion except near the light emission [5]. The supersonic collapse requires sub ns time resolution over a large dynamic range of signals, transcending the capabilities of the typical photomultiplier tubes (PMT) used to detect the scattered light. Previous work used fs pulsed laser scattering to overcome the 2 ns response function of detection PMTs to measure this bubble motion, but was limited by the 2 GHz sampling speed of the digitizer recording the signal [7,8]. Here we report on a new technique combining pulsed Mie light scattering with time correlated single photon counting (TCSPC) [9] for detection of the scattered light which here yields about 50 ps time resolution of the supersonic bubble collapse.

This improved time resolution enables us to determine that the velocity of the bubble's gas-liquid interface reverses from about 0.75 km/sec inward to about 0.2 km/sec outward in less than 250 ps, an acceleration of around  $3.5 \times 10^{12}$  m/s<sup>2</sup> as the bubble contents are compressed nearly to van der Waals hard core densities (Fig. 1). Also by this technique, the beginning of the SL flash (whose Gaussian equivalent duration is resolvable by TCSPC) is found to precede the measured minimum radius of the bubble by about 200 ps. We do not ascribe a physical significance to this time; rather, we propose that it indicates a basic limitation in the use of integrated laser scattering to measure bubble collapse near the time of light emission. The resolution limitations of light scattering measurements may be due to light scattered by the outgoing acoustic "shock" wave around the bubble [1,7,8,10,11] (Fig. 2) as well as variations of the index of refraction of the gas in the bubble away from unity as the density rises dramatically on these time scales so close to

the moment of maximum collapse. For these reasons the actual rate of collapse and acceleration may be greater than those gleaned from the data.

The Mie scattering experiments were conducted on gas bubbles levitated in a spherical, water filled quartz resonator driven at 40 kHz and sealed to control the gas content of the liquid. Light pulses (795 nm, 200 fs, 5 nJ/pulse) were focused onto the bubble from a Ti:sapphire laser running mode locked at 76 MHz. An acousto-optic pulse picker (NEOS N17389) could open a 15 ns window in the path of the laser

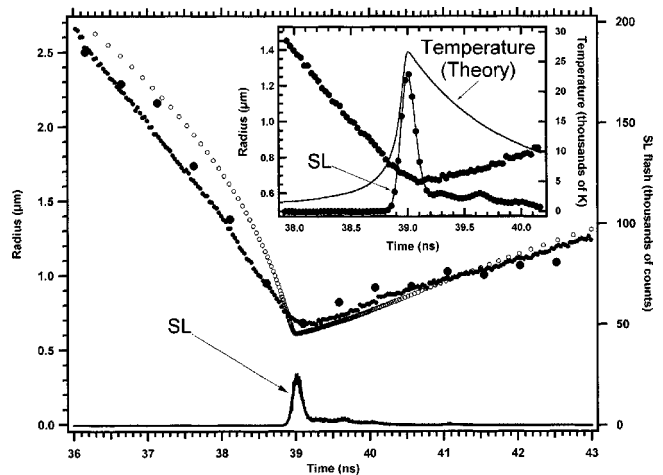


FIG. 1. Time correlated single photon Mie scattering data for 150 torr 1% xenon in oxygen bubble in water (small filled circles). The smooth line is the SL flash measured relative the same time axis, and the large filled circles show pulsed Mie scattering data from Ref. [1] for the same type gas mixture in the same resonator. The open circles are a RP solution with  $R_0=4.1 \mu\text{m}$  and  $P_a=1.45 \text{ atm}$ . (40 kHz) which was the fit to the hydrodynamic motion used to calibrate the data. The inset shows a detail of the relative timing of the measured bubble motion and the SL light emission. The measured SL flash width is 150 ps FWHM which deconvolves using a 45 ps resolution function to a Gaussian equivalent 143 ps. The temperature plotted on the inset is calculated from the RP equation with a uniform van der Waals model described in the text. We show this theoretical temperature because such a uniform bubble model has been proposed for SL [16]. In view of the supersonic collapse of the bubble as well as the emission of the outgoing supersonic acoustic pulse from the bubble (Fig. 2) we question this model.

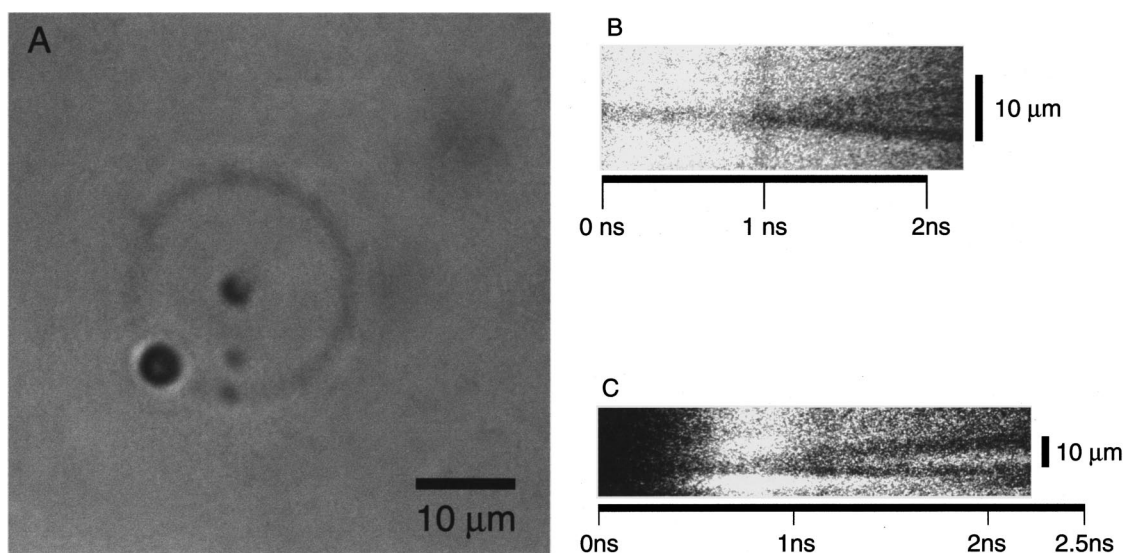


FIG. 2. Emission of an outgoing shock wave from a collapsing bubble (100 torr 1% Xe in oxygen at 40 kHz). (a) Two-dimensional (extinction) shadowgraph photo obtained 5–10 ns after the moment of collapse with a 3 ns flash of light showing a spherical bubble surrounded by the emitted outgoing shockwave. The backlighting source is the fluorescence of Nile Blue A in methanol (0.025% by weight) excited by the 3 ns pulse of a Nd:YAG laser (532 nm). Also visible around the bubble are three particles of dirt which appeared to be trapped to the bubble. The bubble tended to collect such particles; the longer the bubble had existed the more dirt likely to be trapped (only occasionally did such a trapped particle suddenly leave the vicinity of the bubble). These dirt particles appeared at fixed angular locations within an acoustic cycle (following the radial pulsations of the bubble in and out about  $35 \mu\text{m}$  to the maximum radius of the bubble) and smoothly orbited around the bubble on a much slower timescale (0.1 to 10 s). At various drive levels and phases of the acoustic cycle we were unable to resolve aspherical distortions of the bubble. (b) Time resolved single shot (extinction) shadow graph near the minimum radius of a collapsing-rebounding bubble and emitted outgoing pressure pulse obtained by imaging a horizontal cut through the bubble of the image shown in (a) onto the input slit of a streak camera (Hamamatsu C1587 with high speed plug in M1952) with a long distance microscope (Zeiss LD achroplan-20x) and backlighting with the 3 ns pulse of light (described above) during the time sweep [19]. The streak camera slits were set for  $200 \mu\text{m}$  yielding a time resolution function of about 100 ps. The initial speed of the shockwave is about 2.3 km/sec (Mach 1.6 relative to the speed of sound in water). At late times the speed of the outgoing pulse reduces to about Mach 1.0. The line crossing the image at about 1 ns is an artifact of this individual streak camera. (c) Same as (b) but for a bubble driven at 16.5 kHz (Zeiss Achromat S 2.5x) showing a shock wave leaving the bubble at Mach 4 (relative to the speed of sound in water) or greater. Contrast was seen only for the top side of the shockwave due to off-axis alignment of the condenser lens collecting the backlighting onto the bubble.

output to slow the stream of laser pulses. Light from the SL flash was collected by a PMT (Hamamatsu H5783-03), which triggered a delay generator (SRS DG535), used to wait one acoustic period and then trigger the pulse picker to allow one laser pulse to strike the bubble near the minimum radius. Light scattered from the laser pulse by the bubble was collected from around  $60^\circ$  from the forward direction by a 2 in.  $f/1$  lens and was focused through a polarizer (aligned with the laser polarization), a 705 nm long pass glass filter, and a 3 nm full-width at half-maximum (FWHM) interference filter centered at 795 nm onto a microchannel plate (MCP) PMT (Hamamatsu R3809; Quantum efficiency at 795 nm is about 0.18%). Additionally neutral density filters (OD 3) were used to attenuate the light entering the R3809 MCP PMT to generate single photo electron signals. After conditioning with a constant fraction discriminator (CFD) (EG&G Ortec 935) this signal was used to start a time to amplitude converter (TAC) (EG&G Ortec 566).

SL light emitted by the bubble was collected in a direction near the entering laser beam (to minimize the laser scattered light) by a lens onto another MCP PMT (Hamamatsu R2809) with appropriate filters to block the infrared of the laser. An aperture maintained the light level at around 10 photo electrons, which is the level used for timing calibration of the tube. This signal after discriminating in the CFD was used to

stop the TAC. The arrival time of the laser flash wandered around in the pulse picker window since the laser repetition rate and the acoustic frequency were incommensurate. Time intervals between the single photo-electron events in the 3809 and the ‘‘hard trigger’’ SL events in the 2809 were collected from the TAC by a computer into 1.5 ps bins and accumulated to build a statistical sampling of probabilities of detecting a scattering event as a function of time around the SL flash shown in Fig. 3. Because the intensity of a laser flash was modified by its location in the laser window, the laser window profile was measured by reflecting the beam (without a bubble present) from a mirror onto the (3809) MCP (with a difference in path length than bubble scattering of about 2.5 in. or 210 ps which was corrected) and collecting data with the TAC stop signal and laser window trigger generated by an oscillator at 40 kHz. This profile (which is smooth near the minimum bubble radius) was fit to a high-order polynomial (to minimize noise) and used to divide the data.

TCSPC is based on the principle that when in single photon level, the probability as a function of time to detect a photon is proportional to the intensity of light as a function of time. The distribution of 3809 detection probability is thus equated to the intensity of light scattered from the bubble as a function of time. Where the probability of detection was

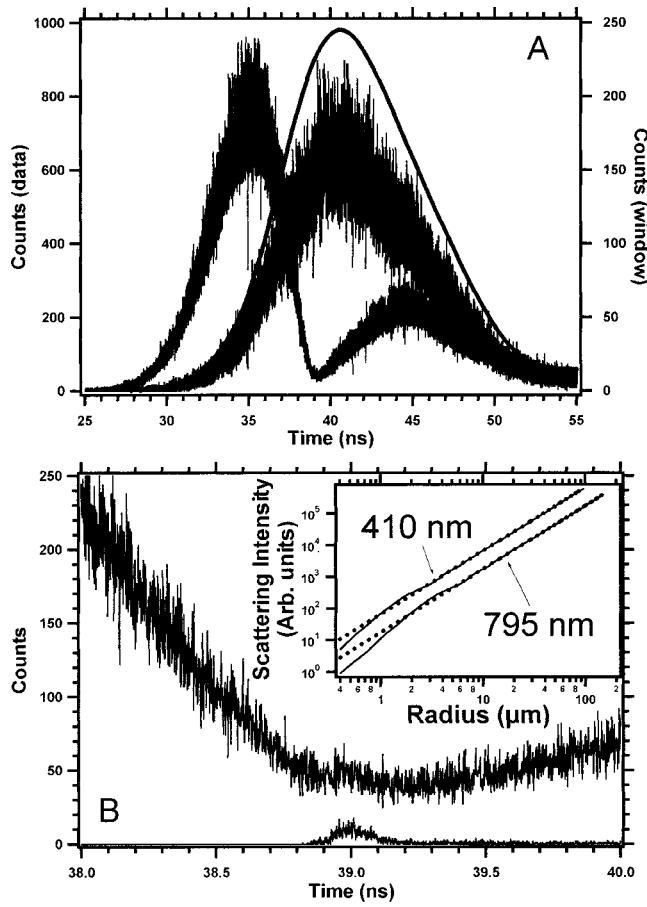


FIG. 3. (a) Raw data (counts per 1.5 ps bin in 1005 s) and laser window measurement (and fit) used to generate the radius vs time curve in Fig. 1. (b) Detail near the minimum radius as well as the SL leaking through the filters which is eventually subtracted. Due to the one acoustic cycle delay in triggering, the laser window is opened every other bubble collapse (20 kHz) giving about 2000 total laser flashes per 1.5 ps bin (for this run). The photo-electron generation rate near the minimum is around 2 or 3% or about 15 scattered photons entering the MCP. Thus, a more precise description of the experiment would be time correlated single *photoelectron* Mie scattering. Inset: Mie scattering calculations for light scattered into a range of angles between 30° and 80° from the forward direction from a bubble in water ( $n_{\text{water}}/n_{\text{bubble}} = 1.33/1.0$ ) for horizontally polarized light as used in the experiment as a function of bubble size. A radius squared curve is also shown which is arranged to match the Mie intensity for a 150  $\mu$  radius.

higher, the intensity is under estimated since a small portion of events will be two-photon events which are interpreted as one-photon events by the discrimination. As the process obeys Poisson statistics the correction factor is given by the intensity

$$I \propto -\ln[1 - (N_{\text{counts/bin}}/N_{\text{flashes/bin}})].$$

By collecting light in a large solid angle, the Mie diffraction effects are smoothed yielding scattering intensity almost proportional to bubble radius squared. Corrections are at most 15% in radius (see Fig. 3 for Mie scattering calculations [12]). The data shown in Fig. 1 were obtained from the scattered intensity by the following procedure. After applying the statistics correction discussed above, the square root of

the data was calculated. For radial calibration, we matched the data from the TCSPC pulsed scattering method to data on the same type of bubble using the pulsed Mie scattering method of Ref. [1] [which is calibrated in radius independently by matching after bounce dynamics to the Rayleigh-Plesset (RP) equation]. This older data was corrected for Mie scattering in the following “look up” method (Fig. 3). For each time bin the intensity suggested by the  $R^2$  approximation was determined for the indicated radius. The Mie calculation was next used to determine what radius would generate that same intensity. That new radius was then assigned to the time bin of interest. The Mie correction to the old data suggests a true  $R_{\text{min}}$  for the bubble. The TCSPC data was scaled so that after the same sort of “look up” Mie corrections its  $R_{\text{min}}$  matched that of the old data.

The timing accuracy of this data is limited by the transit time spread of the 3809 MCP to single photon events which was measured with fs laser flashes to be about 45 ps FWHM. The flash to flash jitter of the SL was measured during this experiment with a time interval meter (SRS 620) triggering on the 2809 output to have FWHM of 100 ps. The jitter in the trigger PMT and the delay generator (about 75 ps) don't affect the data directly because they change the timing of the window opened by the pulse picker.

In the brightest systems, some SL was visible in the scattering data as shown in Fig. 3. To correct the data for this effect the laser was blocked and the amount of SL leaking through the filters during an otherwise identical run was measured and then subtracted from the raw data after which the 1.5 ps time bins were rebinned to 30 ps bins. With the laser blocked and the 795 $\times$ 3 nm and the 705 nm long pass filters removed (resulting in an optical path about 10 ps shorter), the SL flash could also be measured relative to the same time axis as the dynamics. Such a measurement is also shown in Fig. 1 where it is evident that the beginning of the 150 ps FWHM flash precedes the minimum measured radius by about 200 ps.

Shown in Fig. 1 along with the measured data is a solution to the RP equation [13,14]

$$R\ddot{R} + \frac{3}{2}\dot{R}^2 = \frac{1}{\rho}(P_g - P_0 - P_a) - \frac{4\eta\dot{R}}{\rho R} - \frac{2\sigma}{\rho R} + \frac{R}{\rho c} \frac{d}{dt}(P_g - P_a), \quad (1)$$

where  $R$  is the bubble wall,  $c$ ,  $\eta$ ,  $\sigma$ ,  $\rho$  are the sound speed, viscosity, surface tension, and density of the liquid, and  $P_g$ ,  $P_0$ ,  $P_a$  are the pressure of the gas in the bubble, the static pressure, and the acoustic pressure. The terms in  $1/c$  are acoustic radiation terms which have been added as the leading terms of a low mach number expansion of the dynamics [14,15]. The gas inside the bubble is assumed to follow a van der Waals equation of state (including only the hard core contribution ‘ $b$ ’ =  $\frac{4}{3}\pi a^3/N$  when  $N$  is the number of moles in the bubble). Figure 1 shows the temperature predicted by Eq. (1) supplemented with the assumptions of a spatially uniform adiabatic bubble interior so that the temperature is  $T_g(R) = [T_0 R_0^{3(\gamma-1)} / (R^3 - a^3)^{\gamma-1}]$ , where  $\gamma$  is the polytropic index and  $R_0$  is the ambient radius. At the high ve-

locities reported here, the interior should be *nonuniform* so that deviations from this simple model should be significant [14,16].

The factor of 4 decrease in the speed of the bubble wall as it passes through its minimum radius implies that over 90% of the bubble energy is radiated into an outgoing shock wave. Shadowgraph [17] images of the shock wave (Fig. 2) yield [18] Mach numbers greater than 4. According to the Tait equation of state [19] the pressures approach 1 Mbar (for bubbles with  $R_0 \approx 9 \mu\text{m}$ ,  $R_{\text{max}} \approx 90 \mu\text{m}$  driven at 16.5 kHz). The shock wave and micron sized dust particles [20] (that are attracted by the bubble) scatter light out of the incident beam affecting measurements near the minimum radius. These effects indicate fundamental limitations of laser scattering methods to measure the climax of a Rayleigh bubble collapse.

We have reported a technique which achieves a 50 ps

resolution in Mie scattering. This technique, which combines TCSPC light detection with pulsed laser scattering, has been developed with the goal of measuring the dynamical motion of an imploding bubble as it passes through the moment of SL. The 50 ps resolution appears to be shorter than any physical process that can be clearly deconvolved from the data. Deviations from the behavior predicted by the RP equation are apparent, which could be expected since Mach numbers of unity (relative to the liquid sound speed) are approached by the bubble, and surpassed in the theory.

This research was supported by the NSF division of Atomic, Molecular and Optical Physics and DARPA through the ONR. We thank H. Fetterman, P. Marston, and J. Golovchenko for valuable discussions. We thank L. T. Cheng and S. Osher's group for valuable assistance with image enhancement.

- 
- [1] B. P. Barber *et al.*, Phys. Rep. **281**, 65 (1997); S. Putterman, Phys. World **11**, 42 (1998).
- [2] B. Gompf *et al.*, Phys. Rev. Lett. **79**, 1405 (1998); R. A. Hiller *et al.*, *ibid.* **80**, 1090 (1998).
- [3] Lord Rayleigh, Philos. Mag. **34**, 94 (1917).
- [4] B. D. Storey and A. J. Szeri, J. Fluid Mech. **396**, 203 (1999); C. C. Wu and P. H. Roberts, Phys. Rev. Lett. **70**, 3424 (1993); W. C. Moss *et al.*, Phys. Rev. E **59**, 2986 (1999); I. Kondic *et al.*, *ibid.* **52**, 4976 (1995); K. Yausi, *ibid.* **56**, 6750 (1997); S. Hilgenfeldt *et al.*, Nature (London) **398**, 402 (1999); V. Kamath *et al.*, J. Acoust. Soc. Am. **94**, 248 (1993).
- [5] B. P. Barber and S. J. Putterman, Phys. Rev. Lett. **69**, 3839 (1992).
- [6] G. A. Delgadino and F. J. Bonetto, Phys. Rev. E **56**, R6248 (1997).
- [7] K. Weninger *et al.*, Phys. Rev. Lett. **78**, 1799 (1997).
- [8] B. P. Barber *et al.* Philos. Trans. R. Soc. London, Ser. A **355**, 641 (1997).
- [9] D. V. O'Conner and D. Phillips, *Time-Correlated Single Photon Counting* (Academic, New York, 1984).
- [10] T. J. Matula *et al.*, J. Acoust. Soc. Am. **103**, 1377 (1998); J. Holzfuss *et al.*, Phys. Rev. Lett. **81**, 5434 (1998); Z. Q. Wang *et al.*, Phys. Rev. E **59**, 1777 (1999).
- [11] B. Gompf *et al.*, J. Acoust. Soc. Am. **105**, S959 (1999).
- [12] H. C. Van de Hulst, *Light Scattering by Small Particles* (Wiley, New York 1957); J. V. Dave, IBM J. Res. Dev. **13**, 302 (1969); P. L. Marston, Appl. Opt. **30**, 3479 (1991).
- [13] A. Prosperetti, Rendiconti S.I.F. **XCIII**, 145 (1984).
- [14] R. Löfstedt *et al.*, Phys. Fluids A **5**, 2911 (1993).
- [15] A. Prosperetti, J. Fluid Mech. **168**, 457 (1986).
- [16] S. Hilgenfeldt *et al.*, Phys. Fluids **11**, 1318 (1999).
- [17] J. Noack *et al.*, J. Appl. Phys. **83**, 7488 (1998).
- [18] A. Marquina and S. Osher, UCLA Cam Report No. 99-5, 1999 (unpublished).
- [19] C. Hunter, J. Fluid Mech. **8**, 241 (1960).
- [20] W. T. Coakley and W. L. Nyborg, in *Ultrasound: Its Application in Medicine and Biology, Part 1*, edited by F. Fry (Elsevier, Amsterdam, 1978), p. 105; D. L. Miller, J. Acoust. Soc. Am. **84**, 1378 (1988).